

# RESOLVED SPECTROSCOPY OF M DWARF/L DWARF BINARIES. I. DENIS J220002.05–303832.9AB

ADAM J. BURGASSER<sup>1</sup>

Massachusetts Institute of Technology, Kavli Institute for Astrophysics and Space Research, 77 Massachusetts Avenue, Building 37,  
Cambridge, MA 02139-4307, USA; ajb@mit.edu

AND

MICHAEL W. McELWAIN

University of California Los Angeles, Division of Astronomy & Astrophysics, 8965 Math Science Bldg., 405 Hilgard Ave., Los Angeles,  
CA, 90095-1562; mcelwain@astro.ucla.edu

*Accepted to AJ*

## ABSTRACT

We present the discovery of the common proper motion M9 + L0 binary DENIS J220002.05–303832.9AB, identified serendipitously with the SpeX near infrared imager/spectrograph. Spectral types are derived from resolved near infrared spectroscopy of the well-separated ( $1''.09 \pm 0''.06$ ) components and comparison to equivalent data for M and L dwarf spectral standards. Physical association is deduced from the angular proximity of the sources, their common proper motion and their similar spectrophotometric distances ( $35 \pm 2$  pc). The estimated distance of this pair implies a projected separation of  $38 \pm 3$  AU, wider than typical separations for other M dwarf/L dwarf binaries, but consistent with the maximum separation/total system mass trend previously identified by Burgasser et al. (2003). We discuss the DENIS 2200–3038AB system in context with other low mass binaries, and its role in studying dust formation processes and activity trends across the transition between the M and L dwarf spectral classes.

*Subject headings:* binaries: visual — stars: individual (DENIS J220002.05–303832.9) — stars: low mass, brown dwarfs

## 1. INTRODUCTION

Multiple stellar systems are important probes of star formation processes and atmospheric physics, and provide one of the few means of directly measuring stellar mass. Multiples are particularly useful for studying the physical properties and origins of the lowest mass stars and brown dwarfs, the latter being stars of such low mass that they are incapable of sustaining core hydrogen fusion (Kumar 1962; Hayashi & Nakano 1963). Coeval binaries facilitate the study of surface gravity and temperature effects on the complex spectra of cool dwarfs independent of age or metallicity variations, and mass measurements allow specific tests of evolutionary theory (Lane et al. 2001; Bouy et al. 2004; Zapatero Osorio et al. 2004). The multiplicity fraction, separation distribution and mass ratio distribution of low mass binaries provide critical constraints on the current menagerie of formation models (Bouy et al. 2003; Burgasser et al. 2003b; Close et al. 2003).

High resolution imaging surveys of very low mass stellar and brown dwarf systems ( $M_{\text{total}} \lesssim 0.2 M_{\odot}$ ) have been conducted by several groups in recent years, focusing on both field (Koerner et al. 1999; Martín, Brandner & Basri 1999; Reid et al. 2001; Close et al. 2002, 2003; Bouy et al. 2003; Burgasser et al. 2003b; Gizis et al. 2003; Siegler et al. 2003, 2005) and young cluster (Martín et al. 1998, 2000, 2003; Neuhäuser et al. 2002; Pinfield et al. 2003; Kenyon et al. 2005; Kraus, White & Hillenbrand 2005;

Luhman, McLeod & Goldenson 2005) populations. These studies have converged to similar results: very low mass binaries are relatively rare ( $f_{\text{bin}} \sim 10\text{--}20\%$ ) and tend to form closely-separated ( $\rho \lesssim 20$  AU), nearly-equal mass ( $q \equiv M_B/M_A \sim 1$ ) systems. These results lend support for dynamical ejection formation models (Sterzik & Durisen 1998, 2003; Reipurth & Clarke 2001; Bate, Bonnell, & Bromm 2002a,b, 2003; Delgado-Donate, Clarke & Bate 2003; Delgado-Donate et al. 2004; Bate & Bonnell 2005; Umbreit et al. 2005), in which gravitational scattering of protostellar cores prevents both the accretion of significant gas and dust (resulting in low masses) and the integrity of any weakly bound low-mass systems.

However, a handful of widely separated low mass binaries have been identified serendipitously, including GG Tau Bab (Leinert et al. 1991; White et al. 1999), 2MASS J11011926-7732383AB (Luhman 2004, hereafter 2MASS 1101-7732AB) and DENIS J055146.0-443412.2AB (Billeres et al. 2005, hereafter DENIS 0551-4434AB). These systems, containing late-type M and (in the case of DENIS 0551–4434AB) L dwarf components, have projected separations of over 200 AU, more than 10 times wider than the apparent separation limit found in high resolution imaging surveys. The first two binaries, identified in the young associations Taurus Auriga and Chameleon I, contain substellar mass components. DENIS 0551-4434AB is likely composed of two low mass stars. These systems are fragile, with escape velocities  $V_{\text{esc}} \lesssim 1$  km s<sup>−1</sup>, smaller than the  $\sim 2$  km s<sup>−1</sup> velocity dispersions observed in young clusters (Jones & Walker 1988; Joergens & Guenther 2001) and predicted in ejection models (Bate, Bonnell, & Bromm 2003). Both Luhman (2004) and Billeres et al. (2005) argue that

<sup>1</sup> Visiting Astronomer at the Infrared Telescope Facility, which is operated by the University of Hawaii under Cooperative Agreement NCC 5-538 with the National Aeronautics and Space Administration, Office of Space Science, Planetary Astronomy Program.

the existence of such weakly bound systems provides strong evidence that dynamic processes are not the exclusive means of forming the lowest mass stars and brown dwarfs.

In this article, we present the discovery of a new low mass binary, DENIS J220002.05–303832.9AB (hereafter DENIS 2200–3038). Originally identified as an unresolved L0 dwarf by Kendall et al. (2004) in the Deep Near Infrared Survey of the Southern Sky (Epchtein et al. 1997), we find this source to be a well-separated ( $1''.1$ ,  $\sim 40$  AU) M9 + L0 pair. In § 2 we describe our imaging and spectroscopic observations, and data reduction techniques. In § 3 we present analysis of the data, including resolved photometry and spectroscopy of the pair and its systemic properties. Physical association is deduced from the angular proximity, similar spectrophotometric distances and common proper motion of the components. In § 4 we discuss the properties of this system in context with other low mass binaries and its role in the study of atmospheric and activity trends across the M dwarf/L dwarf boundary. Results are summarized in § 5.

## 2. OBSERVATIONS

### 2.1. Imaging

DENIS 2200–3038 was observed on 2004 September 7 (UT) as part of a campaign to acquire low resolution near infrared spectra of late-type comparison stars using the SpeX spectrograph (Rayner et al. 2003), mounted on the 3m NASA Infrared Telescope Facility (IRTF). Conditions during the observations were non-photometric, with light cirrus but excellent seeing ( $0''.6$  at  $J$ -band). Acquisition images with the instrument’s guiding camera revealed two distinct sources at the position of DENIS 2200–3038, separated by roughly  $1''$ . We obtained a series of images of the pair through the Mauna Kea Observatory (MKO)  $JHK$  filter set (Simons & Tokunaga 2002; Tokunaga, Simons & Vacca 2002), interspersed with images of a nearby bright single star 2MASS J22001305–3041415 (2MASS  $J = 12.51 \pm 0.03$ ,  $J - K_s = 0.41 \pm 0.04$ ) as a point spread function (PSF) calibration source. The image rotator was set to  $0^\circ$ . Eight dithered exposures were obtained for each pointing, for a total of 200, 120 and 120 s integration for DENIS 2200–3038 at  $J$ ,  $H$  and  $K$ , respectively. We also obtained twilight and bias exposures two nights later during the same observing campaign.

The imaging data were cleaned using a pixel mask constructed from the bias and twilight frames, then pairwise subtracted and divided by the appropriate flat field image for pixel response calibration. The flat field images were created by bias-subtracting, median-combining and normalizing the twilight exposures. The calibrated images were centered and coadded to produce a mosaic for each filter/pointing combination. Figure 1 displays  $6'' \times 6''$  subsections of the  $JHK$  mosaics for the target and PSF star. The two DENIS 2200–3038 sources are clearly resolved, lying along a north-south axis. The northern source is slightly brighter in all three bands.

We measured the relative astrometry and photometry of the DENIS 2200–3038 pair using an iterative PSF fitting algorithm, as follows. First, for each filter the peak positions and fluxes of the two sources were estimated by summing the columns and rows in the appropriate mosaic

image. A model image was then constructed from two of the reduced PSF images acquired in the same filter, shifting and scaling these images to match the estimated positions and fluxes of the DENIS 2200–3038 sources. This model image was then subtracted from one of the reduced DENIS 2200–3038 images, and residuals (standard deviation in the image) computed. The primary pixel coordinate, secondary pixel coordinate, primary flux and secondary flux in the model image were then adjusted iteratively in steps of 0.1 pixels and 0.01 fraction flux until residuals were minimized, typically of order 1–2% of the source peak flux. This procedure was repeated for each reduced image in a target/PSF pointing set, yielding 32 fits per filter. The mean of the flux ratios<sup>2</sup>, separations ( $\rho$ ) and position angles ( $\phi$ ) for each filter were adopted as the derived values, and their scatter as an estimate of experimental uncertainty. We also included uncertainty in the pixel scale ( $0''.120 \pm 0''.002$  pixel<sup>-1</sup>) and rotator alignment ( $0^\circ 25$ ) in the error budget (J. Rayner, 2005, private communication). Results are listed in Table 1.

To calibrate our fitting routine, we repeated the analysis using simulated binary images constructed from random pairings of the PSF images. The simulated images were constructed so as to match the derived binary parameters for DENIS 2200–3038 for each filter, with some variation to replicate the experimental uncertainties. These images were run through the same routine using a third randomly selected PSF image for the fit, and the derived parameters compared to the input values. A total of 10 000 trials were performed for each filter. Overall, no significant systematic deviations were found in these simulations; however, scatter in the simulated fits was significantly larger than the scatter derived from fits to the data. We adopt the standard deviation among the simulation values as estimates of the systematic uncertainty in our fitting technique; these are listed separately in Table 1.

Second epoch  $J$ -band images of the DENIS 2200–3038 pair and the PSF star were also obtained with SpeX exactly one year later on 2005 September 7 (UT). Conditions during this run were poor, with seeing of  $0''.9$ . Six 10 s dithered exposures were obtained of both fields, and analyzed using the same fitting routine. These observations are discussed in further detail in § 3.2.

### 2.2. Spectroscopy

Spectral data for the two DENIS 2200–3038 sources were obtained on 2004 September 7 (UT) using the SpeX prism dispersed mode, which provides low resolution  $0.7$ – $2.5 \mu\text{m}$  spectra in a single order. For all observations, the  $0''.5$  slit was employed, yielding a spectral resolution  $\lambda/\Delta\lambda \approx 150$  and dispersion across the chip of  $20$ – $30 \text{ \AA pixel}^{-1}$ . Spectra were acquired by setting the image rotator to  $90^\circ$ , so that one source lay in the slit while the other source was positioned orthogonal to the orientation of the slit and used for guiding. Note that the slit was not aligned with the parallactic angle ( $\sim 15^\circ$ ), so some differential color refraction is expected in the reduced

<sup>2</sup> Note that the imaging observations were taken in non-photometric conditions; however, we assume that the relative atmospheric transmission over the small separation of the DENIS 2200–3038 pair was constant, and that atmospheric absorption has minimal effect on the relative flux within each individual filter.

spectrum (see below). Six exposures of 120 s each were obtained for both sources in an ABBA dither pattern along the slit, for a total of 720 s integration per source. The A0 V HD 202025 was observed immediately afterward, at a similar airmass (1.64) and with the slit aligned to the parallactic angle, for flux calibration. Internal flat field and Ar arc lamps were observed for pixel response and wavelength calibration.

All spectral data were reduced using the SpeXtool package, version 3.2 (Cushing, Vacca, & Rayner 2004) using standard settings. First, the images were corrected for linearity, pair-wise subtracted, and divided by the corresponding median-combined flat field image. Spectra were optimally extracted using the default settings for aperture and background source regions, and wavelength calibration was determined from arc lamp and sky emission lines. Multiple spectral observations for each source were then median-combined after scaling the individual spectra to match the highest signal-to-noise observation. Telluric and instrumental response corrections for the science data were determined using the method outlined in Vacca et al. (2003). Line shape kernels were derived from the arc lines. Adjustments were made to the telluric spectra to compensate for differing H I line strengths in the observed A0 V spectrum and pseudo-velocity shifts<sup>3</sup>. Final calibration was made by multiplying the observed target spectrum by the telluric correction spectrum, which includes instrumental response correction through the ratio of the observed A0 V spectrum to a scaled, shifted and deconvolved Kurucz<sup>4</sup> model spectrum of Vega.

Due to the proximity of the two DENIS 2200–3038 sources, some contamination of light from one component could be present in the spectrum of the other component. To estimate this, we calculated the integrated light contribution across the 0''.5 slit for a source separated from the slit center by 1''.1, assuming a wavelength-independent<sup>5</sup> Gaussian PSF with a seeing full width at half maximum of 0''.6. The total contribution is 0.4% of the peak source flux, implying contamination of the northern (southern) spectrum by the southern (northern) source of only 0.3% (0.5%) based on the observed flux ratios. We consider this level of contamination to be negligible for our analysis.

The reduced spectra of the two DENIS 2200–3038 components are shown in Figure 2. Both exhibit near infrared spectral energy distributions consistent with late-type M and early-type L dwarfs, including red optical/near infrared spectral slopes; deep H<sub>2</sub>O absorption bands at 1.4 and 1.9  $\mu\text{m}$ ; strong CO absorption at 2.3  $\mu\text{m}$ ; FeH bands at 0.9, 1.2 and 1.6  $\mu\text{m}$ ; TiO and VO absorption at 0.86, 0.78 and 1.05  $\mu\text{m}$ ; and numerous unresolved atomic lines in the *J*- and *K*-bands. Further discussion on the near infrared spectral characteristics of late-type M and L dwarfs can be found in Jones et al. (1994); Leggett et al. (2000, 2001); Reid et al. (2001); Testi et al. (2001); Geballe et al. (2002); Gorlova et al. (2003); McLean et al. (2003); Knapp et al. (2004);

Nakajima et al. (2004) and Cushing, Rayner & Vacca (2005).

### 3. ANALYSIS

#### 3.1. Spectral Classification

Ideally, the classification of a stellar spectrum is most accurately accomplished by direct comparison of that spectrum to a sequence of pre-defined spectral standards, with data obtained over a similar waveband and resolution (Corbally, Gray & Garrison 1994). Currently, no sequence of *near infrared* spectral standards exist for M and L dwarfs, although several studies have examined methods of classification at these wavelengths (Tokunaga & Kobayashi 1999; Reid et al. 2001; Testi et al. 2001; Burgasser et al. 2002b; Geballe et al. 2002; McLean et al. 2003). As a proxy, we compared the DENIS 2200–3038 spectra to equivalent SpeX prism data (Burgasser et al. 2004b; Burgasser et al. in prep.; Cruz et al. in prep.) for the optical spectral standards (Kirkpatrick, Henry, & McCarthy 1991; Kirkpatrick et al. 1999) VB 10 (M8), LHS 2924 (M9), 2MASS J03454316+2540233 (L0; hereafter 2MASS 0345+2540) and 2MASS J14392836+1929149 (L1). Figure 3 shows a normalized spectral sequence of these standards with the spectra of the DENIS 2200–3038 sources overlain. The brighter northern source matches the spectrum of LHS 2924 quite well across the full spectral range, and in particular shows excellent agreement in the band strengths and overall spectral shape. The spectrum of the southern component, on the other hand, has deeper H<sub>2</sub>O and FeH bands and weaker TiO and VO absorption, and shows more consistency with the spectrum of 2MASS 0345+2540. There are slight discrepancies in the peak *H*- and *K*-band flux peaks, however, with the southern DENIS 2200–3038 source exhibiting a slightly bluer near infrared spectral slope. We attribute this to light loss at longer wavelengths due to differential color refraction. Indeed, *J*–*K<sub>s</sub>* colors synthesized from the spectral data of the northern and southern components are 0.07 and 0.12 mags bluer than those derived from the photometry (see below).

Another common method of classifying cool dwarf spectra is through the use of spectral indices. For the DENIS 2200–3038 sources, we examined indices defined by Reid et al. (2001) and Testi et al. (2001), both based on low resolution near infrared spectral data. The Reid et al. study defines several indices measuring the strengths of H<sub>2</sub>O and CO bands and color ratios in late-type M and L dwarf spectra, and provides spectral type calibrations anchored to optical classifications for their H<sub>2</sub>O-A and H<sub>2</sub>O-B indices (sampling the 1.1 and 1.4  $\mu\text{m}$  H<sub>2</sub>O bands) and the *K*1 index of Tokunaga & Kobayashi (1999) over spectral types M8 to L6. Testi et al. (2001) define six indices sampling H<sub>2</sub>O bands and color ratios, and provide calibrations for these indices over types L0 to L8. Due to apparent color refraction effects in our spectral data, we considered only the four H<sub>2</sub>O indices, and extrapolated the Testi et al. linear spectral type calibrations to incorporate late M dwarf types. Table 2 lists the derived values and associated spectral types for all nine indices. The Reid et al. indices yield mean types of M9 and L0 for the northern and southern components, respectively; while the Testi et al. indices yield types of M9.5 and L0 with somewhat larger scatter. Taking

<sup>3</sup> These shifts, of order 200 km s<sup>−1</sup>, compensate for a slight wavelength shift present in the low resolution Vega model spectrum employed for this mode (M. Cushing, 2005, private communication).

<sup>4</sup> <http://kurucz.harvard.edu/stars.html>.

<sup>5</sup> Seeing measurements on 2004 September 7 (UT) for the PSF star in the *JHK* bands were all 0''.6, so this assumption is valid.

these values in conjunction with the direct spectral comparisons shown in Figure 3, we adopt spectral types of M9 and L0 for the two DENIS 2200–3038 sources, with an uncertainty of  $\pm 0.5$  subclasses.

### 3.2. Is DENIS 2200–3038AB a Bound Pair?

Since the two sources at the position of DENIS 2200–3038 have similar brightnesses and spectral types, it appears quite likely that the pair form a gravitationally bound system. To assess this, we examined a number of tests for association. First, the probability of two similarly-typed low mass stars positioned within  $\sim 1\text{--}2''$  of each other is extremely low. Cruz et al. (2003) identified 53 M9–L0 dwarfs in their search of the Two Micron All Sky Survey (Cutri et al. 2003, hereafter 2MASS) spanning  $16\,350\text{ deg}^2$ , implying a surface density of approximately  $3 \times 10^{-3}\text{ deg}^{-2}$  to a depth of  $J \approx 14.5$ , similar to the individual apparent  $J$  magnitudes of the two DENIS 2200–3038 sources (Table 3; see below). The probability that these two sources are aligned by chance is only  $10^{-9}$ , and can be ruled out statistically with very high confidence.

We also examined the relative spectrophotometric distances of these two sources (assuming that they are each single) to assess whether they lie at the same distance. Table 2 lists individual apparent magnitudes for each source on the 2MASS photometric system, derived from 2MASS  $JHK_s$  photometry of the unresolved pair and our measured flux ratios. The  $J$  magnitudes include a small color correction,  $\Delta J(2MASS) - \Delta J(MKO) = -0.02$ , computed by integrating the 2MASS and MKO filter bandpasses over the observed spectra; color corrections at  $H$  and  $K/K_s$  were found to be negligible. (see also Stephens & Leggett 2004). Dahn et al. (2002) find a linear relation between absolute  $J$ -band magnitude and spectral type for subtypes M6.5 to L8 of  $M_J = 8.38 + 0.341 \times \text{SpT}$ , where  $\text{SpT}(M7) = 7$ ,  $\text{SpT}(L0) = 10$ , etc. This implies that two sources lying at the same distance and differing by a single spectral subclass have  $\Delta M_J = \Delta J = 0.34$ . Our value of  $\Delta J = 0.33 \pm 0.10$  is therefore consistent with the two sources lying at the same distance to within  $0.5 \pm 5\%$ . Spectrophotometric distances from the absolute magnitude/spectral type relations of Cruz et al. (2003) and Vrba et al. (2004) yield consistent results, and we adopt the mean and standard deviation of all of these values,  $35 \pm 2\text{ pc}$ , as our estimated distance to the DENIS 2200–3038 pair<sup>6</sup>.

Finally, we assessed whether the pair share common proper motion by comparing the relative astrometry between our first and second epoch images. The 2005 observations yield  $\rho = 1''.08 \pm 0''.02$  and  $\phi = 177 \pm 2^\circ$  (not including systematic uncertainties), consistent with the 2004 observations. The SuperCosmos Sky Survey (Hambly et al. 2001a,b,c) gives a proper motion for DENIS 2200–3038 in Right Ascension and declination of  $\mu_\alpha \cos \delta = 0''.206 \pm 0''.016\text{ yr}^{-1}$  and  $\mu_\delta =$

$-0''.063 \pm 0''.015\text{ yr}^{-1}$ , respectively. The observed change in the southern component position relative to the northern component between the two epochs, including systematic uncertainties, is  $\Delta \alpha \cos \delta = -0''.01 \pm 0''.09$  and  $\Delta \delta = 0''.01 \pm 0''.09$ , implying common proper motion at the 98.9% confidence level ( $2.3\sigma$ ). If systematic uncertainties are ignored, common proper motion is secure at the  $5\sigma$  level.

Based on these considerations, we confidently claim that the two DENIS 2200–3038 components comprise a physically bound, common proper motion system, which we refer to hereafter as DENIS 2200–3038AB.

### 3.3. Physical Properties of the Components

Using the spectrophotometric distance estimate derived above, we deduce a projected separation for the DENIS 2200–3038AB system of  $\rho = 38 \pm 3\text{ AU}$ . This is rather wide for a very low mass binary, and implies a long orbital period. Component masses were estimated using the solar metallicity evolutionary models of Burrows et al. (1997) for ages of 0.5, 1 and 5 Gyr; and adopting effective temperatures of 2400 and 2300 K for the A and B components, respectively, based on the  $T_{\text{eff}}$ /spectral type relation of Golimowski et al. (2004, uncertainties of  $\sim 100\text{ K}$ ). Derived mass estimates range over  $0.072\text{--}0.085\text{ M}_\odot$  and  $0.069\text{--}0.083\text{ M}_\odot$  for the A and B components, respectively, implying a mass ratio of  $0.96\text{--}0.98$  and a total system mass of  $0.14\text{--}0.17\text{ M}_\odot$ . Hence, the period of this system, assuming a typical semi-major axis  $a = 1.29\rho$  (Fischer & Marcy 1992), is roughly  $750\text{--}1000\text{ yr}$ . DENIS 2200–3038AB is clearly a poor candidate for dynamical mass measurements.

## 4. DISCUSSION

### 4.1. Is DENIS 2200–3038AB a True Wide Binary?

The projected separation of DENIS 2200–3038AB is nearly twice that of most late-type M and L dwarf binaries identified to date, and is comparable to the “wide” binaries 2MASS J12073346-3932539AB (Chauvin et al. 2004, 2005, hereafter 2MASS 1207-3932AB), CFHT-PL18AB (Martín et al. 1998, 2000) and LP 724-37AB (Phan-Bao et al. 2005). However, the separations of these systems are not necessarily inconsistent with survey results. Burgasser et al. (2003b) found that the maximum projected separations of low mass binaries scaled with the total mass as

$$\rho_{\text{max}} = 1400 \times M_{\text{tot}}^2\text{ AU} \quad (1)$$

(see also Close et al. 2003). For DENIS 2200–3038AB, our mass estimates imply  $\rho_{\text{max}} = 27\text{--}40\text{ AU}$ , depending on the age of the system. Hence, the measured separation is close to, but not inconsistent with, the empirical limit of Eqn 1. Similarly, both CFHT-PL18AB and LP 724-37AB, with  $\rho = 35$  and  $33\text{ AU}$  and  $M_{\text{tot}} \approx 0.18$  and  $0.20\text{ M}_\odot$ , respectively, are well-constrained by this relation. Hence, we do not consider any of these binaries to be abnormally wide.

2MASS 1207–3932AB, however, presents a different problem. Its membership in the TW Hydra moving association (Gizis 2002) implies a young age (10 Myr; Webb et al. 1999; Mamajek 2005), and correspondingly low substellar masses for its late-type M and L dwarf components. Current estimates of  $M_{\text{tot}}$  for this system range over  $0.025\text{--}0.030\text{ M}_\odot$  (Chauvin et al. 2004;

<sup>6</sup> Spectrophotometric distances derived from the absolute magnitude/spectral type relations of Tinney, Burgasser, & Kirkpatrick (2003) are not in agreement with these values, yielding  $\sim 21$  and  $\sim 31\text{ pc}$  for the northern and southern DENIS 2200–3038 sources, respectively. This discrepancy is due to the fact that the high-order polynomial fits presented in the Tinney et al. study are derived for types L0 and later, and are poorly constrained for late-type M dwarfs.

Mamajek 2005), implying  $\rho_{max} \approx 1$  AU, far less than its observed separation of  $\sim 40$ –55 AU. Similarly, the 2 Myr Cha I binary 2MASS 1101–7732AB, with an estimated system mass of  $0.075 M_{\odot}$ , is about 30 times wider than the 8 AU limit implied by Eqn. 1; and the 2 Myr Taurus low-mass binary GG TauBab is roughly 6 times wider than the limit for its estimated system mass ( $0.15$ – $0.16 M_{\odot}$ ; White et al. 1999; Mohanty et al. 2003). All three of these systems are quite young, and Mugrauer & Neuhauser (2005) have argued (in the case of 2MASS 1207–3932AB) that such weakly bound systems may not have had time to undergo the gravitational encounters that would eventually tear them apart. On the other hand, all three are found in relative low density associations, so such encounters may be rare. Recent simulations by Bate & Bonnell (2005) have shown that wide low mass systems could form when two nearby but unrelated objects are ejected from a star forming region in the same direction; however, this mechanism is not predicted to occur in low density environments like Taurus Auriga, TW Hydra and Cha I.

Perhaps the most interesting low mass wide binary identified thus far is DENIS 0551–4434AB which, as a field source, is unlikely to have an age less than 10 Myr. While common proper motion has not yet been established for this pair, their angular proximity and similar spectrophotometric distances have been cited as strong evidence for physical association. With a projected separation of 220 AU, similar to GG Tau Bab and 2MASS 1101–7732AB, this system far exceeds the separation limit set down by Eqn. 1. Billeres et al. (2005) have pointed out that this system could be a higher multiple; i.e., either A or B or both could harbor unresolved close companions. However, an equal-mass quadrupole or higher is required to fit Eqn. 1, and this would imply a larger spectrophotometric distance (already estimated at 100 pc) and hence wider projected separation. The possibility of one or both components harboring a cool white dwarf companion (c.f., the triple system LHS 4039, LHS 4040 and APMPM J2354–3316C; Scholz et al. 2004) is constrained by the lack of significant blue optical flux, such that this system would have to be extremely old. Neither of these explanations are particularly appealing.

In short, wide ( $a > 100$  AU) low mass and/or brown dwarf binaries appear to be a reality, but as yet these systems are very young ( $\lesssim 10$  Myr) and/or exceedingly rare. Furthermore, all were identified serendipitously, so it remains unclear as to whether they are merely flukes of circumstance or that the tight separation limit deduced from high resolution imaging surveys (such as Eqn. 1) is not representative of the brown dwarf population as a whole. Either situation has important implications on the formation mechanism of low mass stars and brown dwarfs. Therefore, a targeted deep imaging survey, preferably employing proper motion corroboration, would be valuable.

#### 4.2. A Probe of the M dwarf/L dwarf Transition

A robust empirical characterization of the transition between M and L dwarfs has important repercussions on our understanding of the atmospheres of these objects, in which condensate dust becomes an increasingly (but possibly variable) opacity source (Tsuji, Ohnaka, & Aoki 1996a; Tsuji et al. 1996;

Jones & Tsuji 1997; Burrows & Sharp 1999; Allard et al. 2001; Ackerman & Marley 2001; Cooper et al. 2003). By definition, the beginning of the L dwarf class is marked by waning TiO and VO bands that characterize M dwarfs (Kirkpatrick et al. 1999). These gaseous species are lost to the formation of condensates, including titanates and mineral composites (Lodders 2002), which collectively radiate as a warm blackbody in the near infrared. Other condensate constituents such as Al and Ca are also seen to disappear at the M dwarf/L dwarf boundary (McLean et al. 2003). These trends have been identified amongst samples of field dwarfs, and as such may be blurred by the range of ages, masses and compositions that comprise such samples. Characterizing these trends independent of metallicity or age effects could provide a more accurate picture of condensate formation and other atmospheric processes. Under the assumption of coevolution, well-resolved M dwarf/L dwarf binaries such as DENIS 2200–3038AB enable such studies.

In addition, chromospheric activity, as traced through H $\alpha$  emission, is seen to decrease dramatically among the late-type M and early-type L dwarfs, both in terms of frequency and emission strength (Gizis et al. 2000; West et al. 2004). Theoretical considerations suggest that this trend may be the result of an increasingly neutral, cool upper atmosphere, and the subsequent impedance in transferring plasma to a hot chromosphere (Gelino et al. 2002; Mohanty et al. 2002). However, flaring activity does not disappear in the early L dwarfs (e.g., Hall 2002a,b), and H $\alpha$  emission is seen even in cooler T-type brown dwarfs (Burgasser et al. 2000, 2003a). Gizis et al. (2000) point out that older, more massive L dwarfs are more likely to exhibit H $\alpha$  emission, suggesting a mass dependency. Again, as prior empirical studies have been conducted with heterogeneous field samples, optical spectroscopy and monitoring observations of resolved M dwarf/L dwarf pairs may provide a more precise assessment of quiescent and flaring activity trends across this spectral transition.

#### 5. SUMMARY

We have resolved the field dwarf DENIS 2200–3038AB into an M9 + L0 binary separated by  $1^{\circ}09' \pm 0^{\circ}06'$  ( $38 \pm 3$  AU). Resolved spectroscopy has enabled accurate classification of the components, while physical association is deduced from the angular proximity, similar spectrophotometric distances and common proper motion of the two components. We find that while this system, CFHT-Pl-18AB and LP 724-37AB may be wider than most M and L dwarf binaries discovered to date, all three remain well constrained by empirical separation limit trends deduced from high resolution imaging surveys. This is not the case, however, for the young wide binaries GG Tau Bab, 2MASS 1207–3932AB and 2MASS 1101–7732AB, and the recently identified field pair DENIS 0551–4434AB. These four systems may prove to be exceptions to empirical separation trends, or an indication that these trends do not adequately represent the outcome of low mass star and brown dwarf formation. A dedicated survey is required to address these possibilities. Well-resolved M dwarf/L dwarf binaries such as DENIS 2200–3038AB are valuable for studies of dust formation and activity trends at these spectral types, and characterization of the individual components

of these systems should be done to probe these processes in detail.

The authors would like to thank telescope operator Paul Sears and instrument specialist John Rayner for their assistance during the observations, and our referee Suzanne Hawley for her rapid and thorough review of the original manuscript. We also thank Kelle Cruz for providing SpeX spectral data of 2MASS 0345+2540, and Michael Cushing for consultation on the spectral data reduction. AJB acknowledges useful discussions with Peter Allen, Laird Close, Kelle Cruz, I. Neill Reid and Nick

Siegler during the preparation of the manuscript. This publication makes use of data from the Two Micron All Sky Survey, which is a joint project of the University of Massachusetts and the Infrared Processing and Analysis Center, and funded by the National Aeronautics and Space Administration and the National Science Foundation. 2MASS data were obtained from the NASA/IPAC Infrared Science Archive, which is operated by the Jet Propulsion Laboratory, California Institute of Technology, under contract with the National Aeronautics and Space Administration.

Facilities: IRTF(SpeX)

## REFERENCES

- Ackerman, A. S., & Marley, M. S. 2001, *ApJ*, 556, 872
- Allard, F., Hauschildt, P. H., Alexander, D. R., Tamanai, A., & Schweitzer, A. 2001, *ApJ*, 556, 357
- Bate, M. R., & Bonnell, I. A., 2005, *MNRAS*, 356, 1201
- Bate, M. R., Bonnell, I. A., & Bromm, V. 2002a, *MNRAS*, 332, L65
- . 2002b, *MNRAS*, 336, 705
- . 2003, *MNRAS*, 339, 577
- Billères, M., Delfosse, X., Beuzit, J.-L., Forveille, T., Marchal, L., & Martín, E. L. 2005, in press
- Bouy, H., Brandner, W., Martín, E. L., Delfosse, X., Allard, F., & Basri, G. 2003, *AJ*, 126, 1526
- Bouy, H., Brandner, W., Martín, E. L., Delfosse, X., Allard, F., Baraffe, I., Forveille, T., & Demarco, R. 2004, *A&A*, 424, 213
- Burgasser, A. J., Kirkpatrick, J. D., Liebert, J., & Burrows, A. 2003a, *ApJ*, 594, 510
- Burgasser, A. J., Kirkpatrick, J. D., Reid, I. N., Brown, M. E., Miskey, C. L., & Gizis, J. E. 2003b, *ApJ*, 586, 512
- Burgasser, A. J., Kirkpatrick, J. D., Reid, I. N., Liebert, J., Gizis, J. E., & Brown, M. E. 2000a, *AJ*, 120, 473
- Burgasser, A. J., Marley, M. S., Ackerman, A. S., Saumon, D., Lodders, K., Dahn, C. C., Harris, H. C., & Kirkpatrick, J. D. 2002a, *ApJ*, 571, L151
- Burgasser, A. J., McElwain, M. W., Kirkpatrick, J. D., Cruz, K. L., Tinney, C. G., & Reid, I. N. 2004, *AJ*, 127, 2856
- Burgasser, A. J., et al. 2002b, *ApJ*, 564, 421
- Burrows, A., & Sharp, C. M. 1999, *ApJ*, 512, 843
- Burrows, A., et al. 1997, *ApJ*, 491, 856
- Chauvin, G., Lagrange, A.-M., Dumas, C., Zuckerman, B., Mouillet, D., Song, I., Beuzit, J.-L., & Lowrance, P. 2004, *A&A*, 425, L29
- . 2005, *A&A*, 438, L25
- Close, L. M., Siegler, N., Freed, M., & Biller, B. 2003, *ApJ*, 587, 407
- Close, L. M., Siegler, N., Potter, D., Brandner, W., & Liebert, J. 2002, *ApJ*, 567, L53
- Cooper, C. S., Sudarsky, D., Milson, J. A., Lunine, J. I., & Burrows, A. 2003, *ApJ*, 586, 1320
- Corbally, C. J., Gray, R. O., & Garrison, R. F. 1994, *The MK process at 50 years. A Powerful Tool for Astrophysical Insight* (San Francisco: Astronomical Society of the Pacific)
- Cruz, K. L., Reid, I. N., Liebert, J., Kirkpatrick, J. D., & Lowrance, P. J. 2003, *AJ*, 126, 2421
- Cushing, M. C., Vacca, W. D., & Rayner, J. T. 2004, *PASP*, 116, 362
- Cushing, M. C., Rayner, J. T., & Vacca, W. D. 2005, *ApJ*, 623, 1115
- Cutri, R. M., et al. 2003, *Explanatory Supplement to the 2MASS All Sky Data Release*, <http://www.ipac.caltech.edu/2mass/releases/allsky/doc/explsup.htm>
- Dahn, C. C., et al. 2002, *AJ*, 124, 1170
- Delgado-Donate, E. J., Clarke, C. J., & Bate, M. R. 2003, *MNRAS*, 342, 926
- Delgado-Donate, E. J., Clarke, C. J., Bate, M. R., & Hodgkin, S. T. 2004, *MNRAS*, 347, 759
- Epchtein, N., et al. 1997, *The Messenger*, 87, 27
- Fischer, D. A., & Marcy, G. W. 1991, *ApJ*, 396, 178
- Geballe, T. R., et al. 2002, *ApJ*, 564, 466
- Gelino, C. R., Marley, M. S., Holtzman, J. A., Ackerman, A. S., & Lodders, K. 2002, *ApJ*, 577, 433
- Gizis, J. E. 2002, *ApJ*, 575, 484
- Gizis, J. E., Monet, D. G., Reid, I. N., Kirkpatrick, J. D., Liebert, J., & Williams, R. 2000, *AJ*, 120, 1085
- Gizis, J. E., Reid, I. N., Knapp, G. R., Liebert, J., Kirkpatrick, J. D., Koerner, D. W., & Burgasser, A. J. 2003, *AJ*, 125, 3302
- Golimowski, D. A., et al. 2004, *AJ*, 127, 3516
- Gorlova, N. I., Meyer, M. R., Rieke, G. H., & Liebert, J. 2003, *ApJ*, 593, 1074
- Hall, P. B. 2002a, *ApJ*, 564, L89
- . 2002b, *ApJ*, 580, L77
- Hambly, N. C., Davenhall, A. C., Irwin, M. J., & MacGillivray, H. T. 2001a, *MNRAS*, 326, 1315
- Hambly, N. C., Irwin, M. J., & MacGillivray, H. T. 2001b, *MNRAS*, 326, 1295
- Hambly, N. C., MacGillivray, H. T., Read, M. A., et al. 2001c, *MNRAS*, 326, 1279
- Hayashi, C., & Nakano, T. 1963, *Prog. Theo. Physics*, 30, 4
- Joergens, V., & Guenther, E. 2001, *A&A*, 384, 999
- Jones, H. R. A., Longmore, A. J., Jameson, R. F., & Mountain, C. M. 1994, *MNRAS*, 267, 413
- Jones, H. R. A., & Tsuji, T. 1997, *ApJ*, 480, L39
- Jones, B. F., & Walker, M. F. 1988, *AJ*, 95, 1755
- Kirkpatrick, J. D., Henry, T. J., & McCarthy, D. W., Jr. 1991, *ApJS*, 77, 417
- Kirkpatrick, J. D., Reid, I. N., Liebert, J., Gizis, J. E., Burgasser, A. J., Monet, D. G., Dahn, C. C., Nelson, B., & Williams, R. J. 2000, *AJ*, 120, 447
- Kirkpatrick, J. D., et al. 1999, *ApJ*, 519, 802
- Kendall, T. R., Delfosse, X., Martín, E. L., & Forveille, T. 2004, *A&A*, 416, L17
- Kenyon, M. J., Jeffries, R. D., Naylor, T., Oliveira, J. M., & Maxted, P. F. L. 2005, *MNRAS*, 356, 89
- Knapp, G., et al. 2004, *ApJ*, 127, 3553
- Koerner, D. W., Kirkpatrick, J. D., McElwain, M. W., & Bonaventura, N. R. 1999, *ApJ*, 526, L25
- Kraus, A. L., White, R. J., & Hillenbrand, L. A. 2005, *ApJ*, in press
- Kumar, S. S. 1962, *AJ*, 67, 579
- Lane, B. F., Zapatero Osorio, M. R., Britton, M. C., Martín, E. L., & Kulkarni, S. R. 2001, *ApJ*, 560, 390
- Leggett, S. K., Allard, F., Berriman, G., Dahn, C. C., & Hauschildt, P. H. 1996, *ApJS*, 104, 117
- Leggett, S. K., Allard, F., Dahn, C., Hauschildt, P. H., Kerr, T. H., & Rayner, J. 2000, *ApJ*, 535, 965
- Leggett, S. K., Allard, F., Geballe, T., Hauschildt, P. H., & Schweitzer, A. 2001, *ApJ*, 548, 908
- Leinert, Ch., Haas, M., Mundt, R., Richichi, A., & Zinnecker, H. 1991, *A&A*, 250, 407
- Lodders, K. 2002, *ApJ*, 577, 974
- Luhman, K. L. 2004, *ApJ*, 614, 398
- Luhman, K. L., D'Alessio, P., Calvet, N., Allen, L. E., Hartmann, L., Megeath, S. T., Myers, P. C., & Fazio, G. G. 2005, *ApJ*, 620, L51
- Luhman, K. L., McLeod, K. K., & Goldenson, N. 2005, *ApJ*, 623, 1141
- Mamajek, E. E. 2005, *ApJ*, in press
- Martín, E. L., Barrado y Navascués, D., Baraffe, I., Bouy, H., & Dahn, S. 2003, *ApJ*, 594, 525
- Martín, E. L., Brandner, W., & Basri, G. 1999, *Science*, 283, 1718

- Martín, E. L., Brandner, W., Bouvier, J., Luhman, K. L., Stauffer, J., Basri, G., Zapatero Osorio, M. R., & Barrado y Navascués, D. 2000, *ApJ*, 543, 299
- Martín, E. L., et al. 1998, *ApJ*, 509, L113
- McLean, I. S., McGovern, M. R., Burgasser, A. J., Kirkpatrick, J. D., Prato, L., & Kim, S. 2003, *ApJ*, 596, 561
- Mohanty, S., Basri, G., Shu, F., Allard, F., & Chabrier, G. 2002, *ApJ*, 572, 469
- Mohanty, S., Jayawardhana, R., & Barrado y Navascués, D. 2003, *ApJ*, 593, L109
- Mugrauer, M., & Neuhäuser, R. 2005, *AN*, in press
- Muzerolle, J., Hillenbrand, L., Calvet, N., Briceño, C., & Hartmann, L. 2003, *ApJ*, 592, 266
- Nakajima, T., Tsuji, T., & Yanagisawa, K. 2004, *ApJ*, 607, 499
- Natta, A., & Testi, L. 2001, *A&A*, 376, L22
- Neuhäuser, R., Brandner, W., Alves, J., Joergens, V., & Comerón, F. 2002, *A&A*, 384, 999
- Phan-Bao, N., Martín, E. L., Reylé, C., Forveille, T., & Lim, J. 2005, *A&A*, 439, L19
- Pinfield, D. J., Dobbie, P. D., Jameson, R. F., Steele, I. A., Jones, H. R. A., & Katsiyannis, A. C. 2003, *MNRAS*, 342, 1241
- Rayner, J. T., Toomey, D. W., Onaka, P. M., Denault, A. J., Stahlberger, W. E., Vacca, W. D., Cushing, M. C., & Wang, S. 2003, *PASP*, 155, 362
- Reid, I. N., Gizis, J. E., Kirkpatrick, J. D., & Koerner, D. 2001, *AJ*, 121, 489
- Reipurth, B., & Clarke, C. 2001, *AJ*, 122, 432
- Scholz, R.-D., Lodieu, N., Ibata, R., Bienaymé, O., Irwin, M., McCaughrean, M. J., & Schwöpe, A. 2004, *MNRAS*, 347, 685
- Siegler, N., Close, L. M., Cruz, K. L., Martín, E. L., & Reid, I. N. 2005, *ApJ*, 621, 1023
- Siegler, N., Close, L. M., Mamajek, E. E., & Freed, M. 2003, *ApJ*, 598, 1256
- Simons, D. A., & Tokunaga, A. T. 2002, *PASP*, 114, 169
- Sterzik, M. F., & Durisen, R. H. 1998, *A&A*, 339, 95
- . 2003, *A&A*, 400, 1031
- Testi, L., et al. 2001, *ApJ*, 522, L147
- Tinney, C. G., Burgasser, A. J., & Kirkpatrick, J. D. 2003, *AJ*, 126, 975
- Tokunaga, A. T., & Kobayashi, N. 1999, *AJ*, 117, 1010
- Tokunaga, A. T., Simons, D. A., & Vacca, W. D. 2002, *PASP*, 114, 180
- Tsuji, T., Ohnaka, K., & Aoki, W. 1996, *A&A*, 305, L1
- Tsuji, T., Ohnaka, K., Aoki, W., & Nakajima, T. 1996, *A&A*, 308, L29
- Umbreit, S., Burkert, A., Henning, T., Mikkola, S., & Spurzem, R. 2003, *ApJ*, 623, 940
- Vacca, W. D., Cushing, M. C., & Rayner, J. T. 2003, *PASP*, 155, 389
- Vrba, F. J., et al. 2004, *AJ*, 127, 2948
- Webb, R. A., Zuckerman, B., Platais, I., Patience, J., White, R. J., Schwartz, M. J., & McCarthy, C. 1999, *ApJ*, 512, L63
- West, A. A., et al. 2004, *AJ*, 128, 426
- White, R. D., Ghez, A. M., Reid, I. N., & Schultz, G. 1999, *ApJ*, 520, 811
- Zapatero Osorio, M. R., Lane, B. F., Pavlenko, Ya., Martín, E. L., Britton, M., & Kulkarni, S. R. 2004, *ApJ*, 615, 958

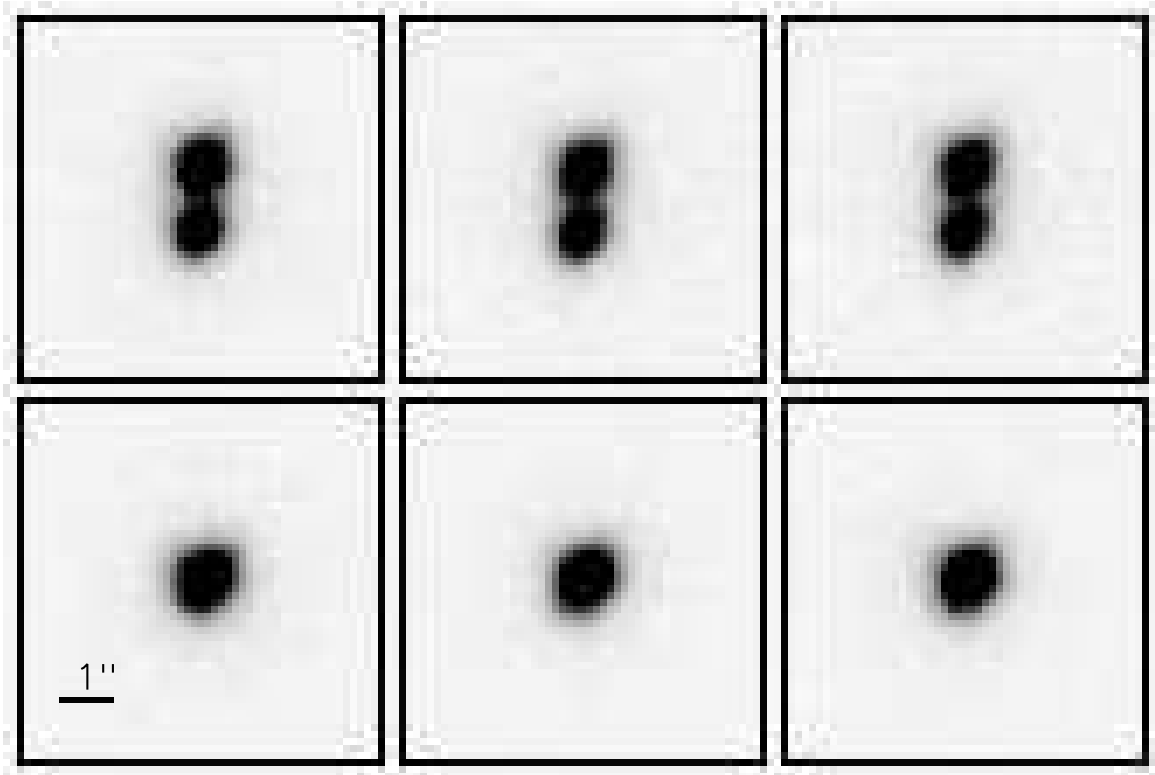


FIG. 1.— Reduced mosaic images of DENIS J220002.05–303832.9AB (top) and the PSF calibrator 2MASS J22001305–3041415 (bottom) in the  $J$ - (left),  $H$ - (middle) and  $K$ -bands (right). Images are  $6''$  on a side, oriented with north at the top and east to the left.



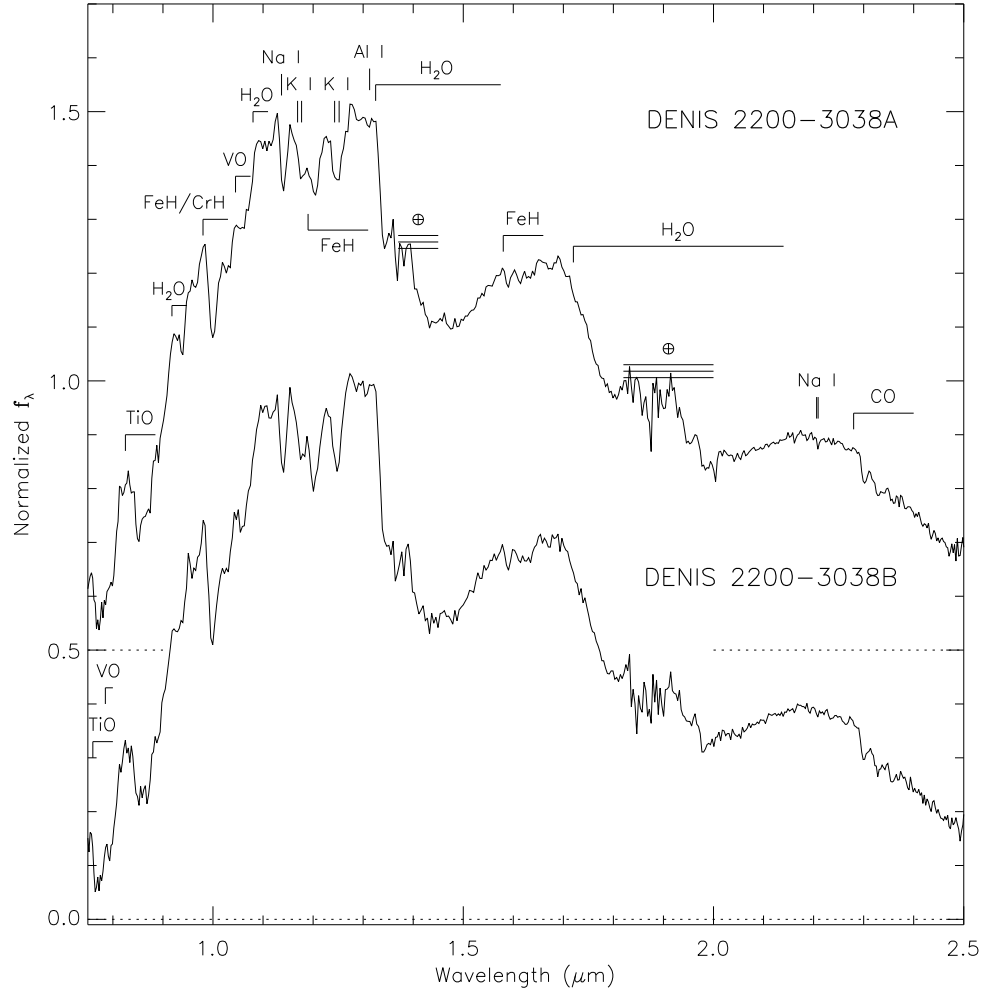


FIG. 2.— Near infrared SpeX spectra of DENIS 2200–3038A (top) and B (bottom). Data are normalized at  $1.28 \mu\text{m}$ , with DENIS 2200–3038A offset by a constant for clarity. Major molecular (TiO, VO, FeH, CrH, H<sub>2</sub>O, CO) and atomic (Na I, K I, Al I) absorption features are labelled, as well as regions of strong telluric absorption ( $\oplus$ ).

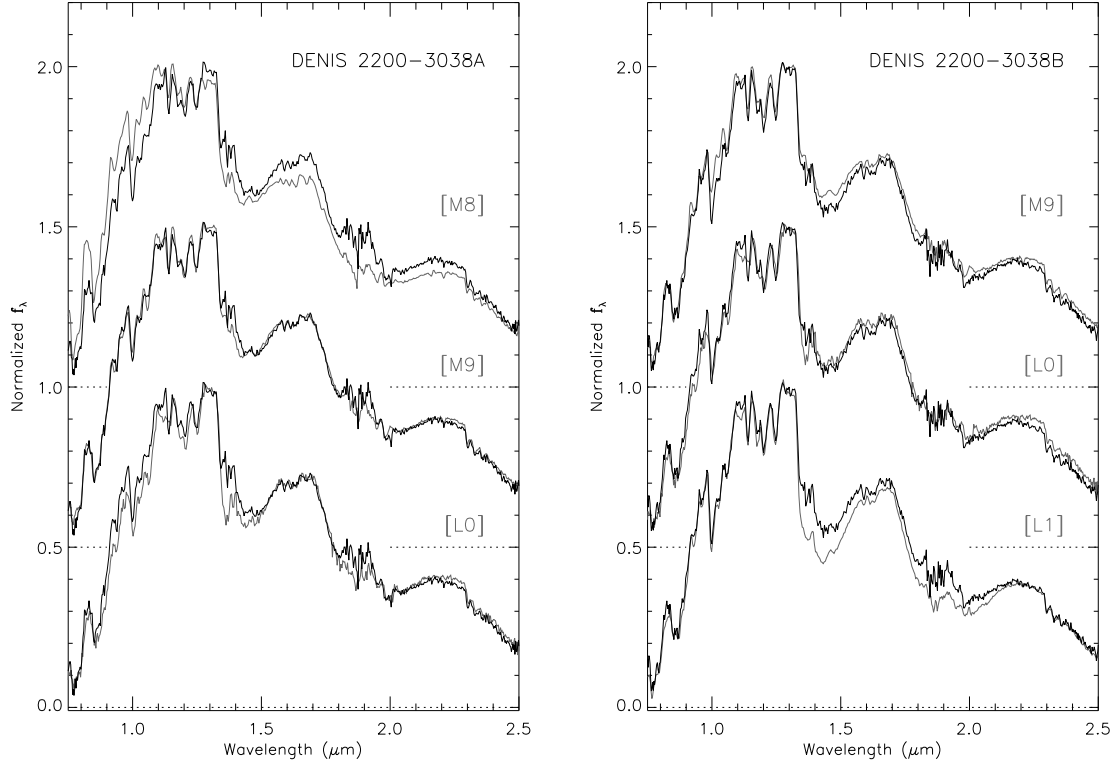


FIG. 3.— Comparison of the near infrared spectra of DENIS 2200-3038A and B (heavy black lines in left and right panels, respectively) to equivalent data (grey lines) for the optical spectral standards VB 10 (M8), LHS 2924 (M9), 2MASS J03454316+2540233 (L0) and 2MASS J14392836+1929149 (L1). All spectra have been normalized at  $1.28 \mu\text{m}$  and offset by constants.

TABLE 1  
PROPERTIES OF DENIS J220002.05–303832.9AB.

Parameter	Value	Ref
$\alpha^a$	$22^h00^m02^s.01$	1
$\delta^a$	$-30^\circ38'32''.7$	1
$\mu$	$0''.22 \pm 0''.05 \text{ yr}^{-1}$	2
$\theta$	$107 \pm 4^\circ$	2
$d$	$35 \pm 2 \text{ pc}$	3
$\rho$	$1''.094 \pm 0''.003 \pm 0''.060^b$	3
	$38 \pm 3 \text{ AU}$	3
$\phi$	$176^\circ 7 \pm 0^\circ 3 \pm 2^\circ 0^b$	3
$J^c$	$13.44 \pm 0.03 \text{ mag}$	1
$H^c$	$12.66 \pm 0.03 \text{ mag}$	1
$K_s^c$	$12.20 \pm 0.03 \text{ mag}$	1
$\Delta J$	$0.328 \pm 0.018 \pm 0.100^b \text{ mag}$	3
$\Delta H$	$0.290 \pm 0.011 \pm 0.090^b \text{ mag}$	3
$\Delta K$	$0.252 \pm 0.015 \pm 0.080^b \text{ mag}$	3
$M_{total}^d$	$0.14\text{--}0.17 \text{ M}_\odot$	3,4
$q^d$	$0.96\text{--}0.98$	3,4
Period <sup>d</sup>	$\sim 750\text{--}1000 \text{ yr}$	3,4

REFERENCES. — (1) 2MASS (Cutri et al. 2003); (2) SuperCosmos Sky Survey (Hambly et al. 2001a,b,c); (3) This paper; (4) Burrows et al. (1997).

<sup>a</sup>Equinox J2000 coordinates at epoch 1998.61 from 2MASS.

<sup>b</sup>Estimates of systematic uncertainty based on PSF fitting simulations; see § 2.1.

<sup>c</sup>2MASS photometry of combined (unresolved) system.

<sup>d</sup>Assuming an age of 0.5–5 Gyr.

TABLE 2  
SPECTRAL CLASSIFICATION INDICES

Index	DENIS 2200–3038A		DENIS 2200–3038B	
	Value	SpT	Value	SpT
Reid et al. (2001)				
H <sub>2</sub> O-A	0.789	M8	0.741	M9.5
H <sub>2</sub> O-B	0.869	M9	0.831	L0
K1 <sup>a</sup>	0.088	M9	0.125	L0
Testi et al. (2001)				
sH <sub>2</sub> O <sup>J</sup>	0.040	L0.5	0.049	L0.5
sH <sub>2</sub> O <sup>H1</sup>	0.152	M9.5	0.203	L0
sH <sub>2</sub> O <sup>H2</sup>	0.370	L0.5	0.389	L1
sH <sub>2</sub> O <sup>K</sup>	0.074	M7.5	0.126	M9

<sup>a</sup>Index defined in Tokunaga & Kobayashi (1999).

TABLE 3  
PROPERTIES OF THE DENIS J220002.05–303832.9AB COMPONENTS

Component	SpT	$T_{eff}^a$ (K)	2MASS			Estimated Mass <sup>b</sup>		
			$J$	$H$	$K_s$	0.5 Gyr ( $M_\odot$ )	1 Gyr ( $M_\odot$ )	5 Gyr ( $M_\odot$ )
DENIS 2200–3038A	M9	2400	$14.05 \pm 0.10$	$13.28 \pm 0.10$	$12.83 \pm 0.10$	0.072	0.079	0.085
DENIS 2200–3038B	L0	2300	$14.36 \pm 0.10$	$13.57 \pm 0.10$	$13.09 \pm 0.10$	0.069	0.077	0.083

<sup>a</sup> $T_{eff}$  estimated from the  $T_{eff}$ /spectral type relation of Golimowski et al. (2004).

<sup>b</sup>Based on the solar metallicity models of Burrows et al. (1997).